Other Supplementary material

Amitosh Dash[1]†, Arjun Anantharaman[1] and Christian Poelma[1]‡

[1]Multiphase Systems (Process & Energy), Mechanical, Maritime and Materials Engineering, Delft University of Technology, Mekelweg 2, 2628CD, Delft, The Netherlands

In this document, we extensively validate single-phase flow results as part of the study in the manuscript titled "**Particle-laden Taylor-Couette flows: Higher order transitions and evidence for azimuthally localized Wavy vortices**". The flow generated in the present facility by the motion of the inner cylinder has been validated in the past for single-phase flows, albeit only with the aid of torque measurements in the study by Ravelet *et al.* (2010). The system has since then been primarily utilized in studies pertaining to highly turbulent flows (thus Reynolds numbers $> 10^4$), with the exception of Alidai *et al.* (2016) who studied turbulent patches for pure outer cylinder rotation. Since the focus of the current study is on inner-cylinder driven, non-turbulent flow regimes, we validate the single-phase flow regimes in our system, primarily with the aid of flow visualization in section 1 and briefly with torque measurements in section 2.

1. Regime classification per flow visualization

As emphasized in the manuscript, single-phase flows in the Taylor-Couette geometry have been studied in much detail previously. For the purpose of this study, we classify the flow regimes into two domains: lower order transitions and higher order transitions. The former is associated with flow regimes appearing between laminar Couette flow and the first fully-formed laminar wavy vortices along the circumferential direction, whereas the latter is associated with flow transitions and flow states that appear beyond. A similar distinction was made by Dutcher & Muller (2009).

1.1. *Lower order transitions: From Laminar Couette Flow to Wavy Vortex Flow*

The lower order transitions are pretty well studied and for single-phase flows, the flow undergoes a transition from purely circular, Couette flow to Wavy Vortex Flow via the regime of Taylor Vortex Flow. We observe this expected behaviour, as exemplified by the images in figure 1.

The flow initially is circular, which is free of any distinct features (figure 1(*a*)), owing to the fact that the flow is purely along the azimuthal direction. Beyond a critical Re, we observe the presence of the Taylor Vortex Flow regime (figure 1(*c*)), where the Taylor vortices appear as steady bands. This regime is often preceded by a regime where bulk of the flow is laminar but vortices due to Ekman pumping are prominent at the ends of the setup (figure 1(*b*)). We observe a more persistent presence of these end vortices in the ramp-up experiments as compared to the ramp-down ones.

In the ramp-up (alternatively, ramp-down) experiments, we observe the first (last) appearance of weak/developing Taylor vortices at $Re = 136$ ($Re = 128$), while they first (last) appear fully developed at $Re = 152$ ($Re = 152$). These are comparable to critical Reynolds numbers predicted by linear stability theory (Di Prima & Swinney 1981, table 6.2) or other analytic expressions (Esser & Grossmann 1996, equation 7), $Re \sim 145$ for

† Email address for correspondence: a.dash@tudelft.nl
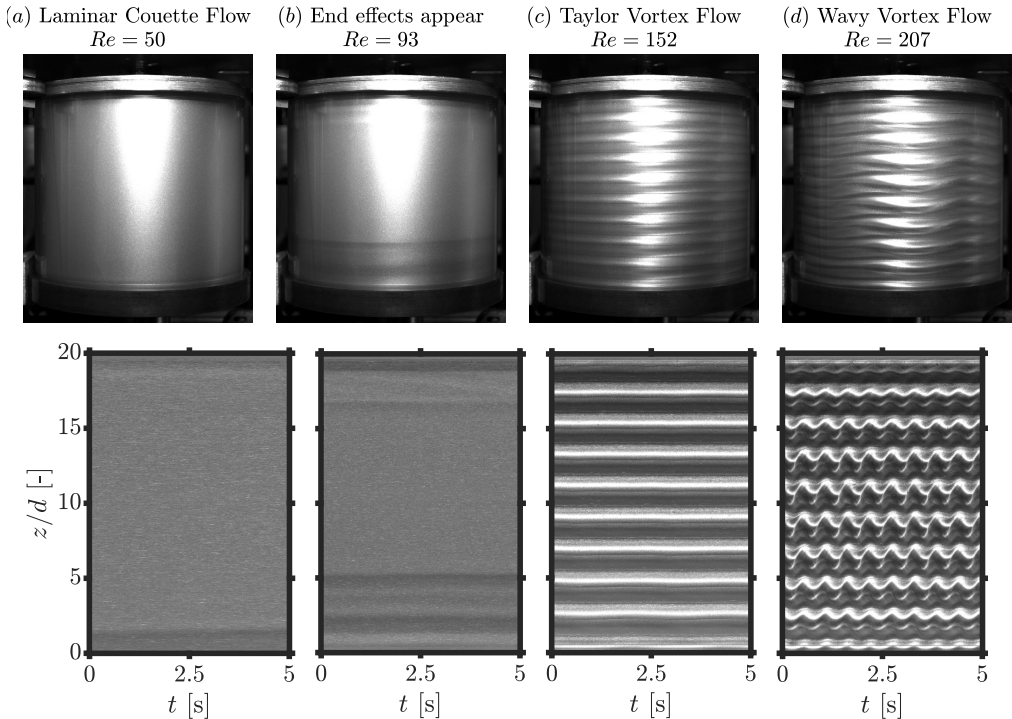‡ Email address for correspondence: c.poelma@tudelft.nl

FIGURE 1. Lower order transitions for single-phase flows. (*Top*) Full field-of-view snapshots (inner cylinder rotates from right to left) (*Bottom*) Corresponding space-time plots (*a*) Circular Couette Flow (CCF). (*b*) Appearance of vortices due to Ekman pumping. (*c*) Taylor Vortex Flow (TVF). (*d*) Wavy Vortex Flow (WVF). Examples belong to the ramp-up experiment and the Reynolds numbers are not indicative of critical values for transition.

a similar geometry. The finite step size in our experimental protocol prevents us from finding the exact boundary of the transition between flow regimes, and for now, we take the critical Reynolds number as $Re_c = 142 \pm 12$. With this, we also believe that the finite length of the cylinders do not significantly impact the critical Re at which the Taylor vortices appear, and this postulation is also in line with the findings of Cole (1976), who did not observe an effect of the aspect ratio on the critical Reynolds number ($\eta = 0.914, 1.23 \leqslant \Gamma \leqslant 61$). One critical difference between the two protocols is the axial wavelength of the vortices. For the ramp-up experiments, pairs of vortices appear to be separated by a distance of $\approx 2.1d$, which deviates slightly from the theoretically expected value of $\approx 2d$. The slight discrepancy may be attributed to the limited resolution in imaging ($\approx 0.14d$) as well as the influence of the end vortices. In contrast, the ramp-down experiments showed the Taylor vortex flow state to have a higher axial wavelength ($\approx 2.32d$), corresponding to a reduction by one Taylor vortex pair. Another factor that could play a role in our observations is the time needed for the onset (alternatively, decay) of Taylor vortices which are estimated to be $Ld/\nu = 50$ s ($10d^2/\nu = 108$ s for decay) by Czarny & Lueptow (2007), compared with the time we spend at a constant shear rate i.e. 90 s. However, these time scales are more appropriate when the Reynolds number under consideration is extremely close to the critical value, which is not applicable to our results owing to the finite step sizes taken.

The critical Reynolds number for transition between Taylor Vortex Flow and Wavy Vortex Flow is found to be between $172 \leqslant Re \leqslant 191$ ($192 \geqslant Re \geqslant 171$) for the ramp-up

(ramp-down) experiments, which suggests that the flow hysteresis does not have a strong influence on the critical point for this transition. We approximate the critical Reynolds number for this transition to be around $Re = 181.5 \pm 10.5$ or $Re/Re_c = 1.28 \pm 0.07$. This is slightly higher than the value of $Re/Re_c = 1.17 \pm 0.02$ reported by Dutcher & Muller (2009) for their system ($\eta = 0.912, \Gamma = 60.7$). This discrepancy may be attributed to the the lower aspect ratio in the current facility. Cole (1976) showed that a reduction in the aspect ratio led to an increase in the critical Reynolds number for the transition between Taylor Vortex Flow and Wavy Vortex Flow, due to the damping provided by the ends (Jones 1985).

1.2. *Higher order transitions: From Laminar Wavy Vortices to Turbulent Taylor Vortices*

The higher order transitions in single-phase Taylor-Couette flow are also well established and we adopt the conventions of Dutcher & Muller (2009) as the basis for our classification. The following flow regimes are identified on the basis of the temporal spectrum: Wavy Vortex Flow, when the spectrum shows a single, distinctly identifiable peak; Modulated Wavy Vortex Flow, when the spectrum shows multiple, incommensurate, distinctly identifiable peaks in the spectrum; Chaotic Wavy Vortex flow, when the spectrum also has multiple peaks and the flow also shows small-scale structures; Wavy Turbulent Vortex Flow, when the flow appears to have small-scale structures but the spectrum has a single, dominant peak, and; Turbulent Taylor Vortex Flow, when the Taylor vortices appear to be completely turbulent and the spectrum has no distinct peaks. The Chaotic Wavy Vortex Flow regime has also been referred to as "weakly turbulent" (Fenstermacher *et al.* 1979) and "Turbulent modulated wavy vortices" (Lueptow *et al.* 1992).

Examples of the different flow regimes and their corresponding spectra can be seen in figure 2. The primary tool we employ is a simple spectral analysis along the time-axis of the space-time plots. The spectra along each axial location are averaged to return a single spectrum. The averaging is not expected to be detrimental as fundamental frequencies have been found to be independent of the axial location (Fenstermacher *et al.* 1979), even though this might not hold true for the amplitudes (see figure 1(d), for example). Peaks in the spectra are identified as follows: All points at least ten median average deviations away from the median of the spectrum are marked as "potential peaks". Hereafter, only the "potential peaks" that are local maxima in the neighbourhood of five points are retained as true peaks. The frequencies in the spectra are normalized by the rotational frequency of the inner cylinder (f_i). Thus, all peaks close to $f/f_i = 1$ may be associated with the system itself (Dutcher & Muller 2009). We do not perform an extremely detailed, quantitative analysis of the spectra (for example, identifying the significance of different peaks, and identifying all the linear combinations), as it is not trivial (as evidenced by Gorman *et al.* 1980; Takeda *et al.* 1993, in table 3 and figure 2 respectively) while also going beyond the scope of the current study.

While a similar spectral analysis can also be performed along the space-axis to yield axial wavenumbers, we restrict our discussion from the perspective of (de)generation of vortex pairs (also referred to as vortex pinching/splitting processes by King & Swinney (1983)). Given that our system has two fixed end plates, which fix the boundary conditions for the flow, the (de)generation of vortices in the axial direction only occurs in pairs. Azimuthal wavenumbers can be estimated with the help of full field-of-view snapshots, with the knowledge that only integer number of waves may be present along the circumference, as well as the ansatz that wave speeds do not change significantly upon a small variation in the Reynolds number (see King *et al.* 1984, figure 7).
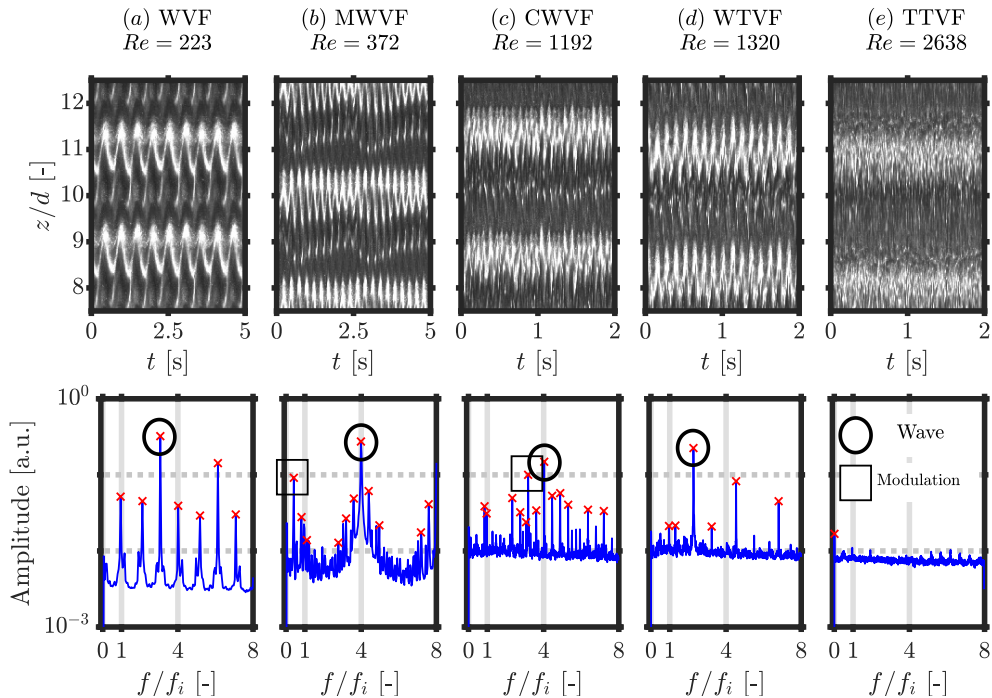
FIGURE 2. Higher order transitions for single-phase flows. (*Top*) Detailed portions of space-time plots. (*Bottom*) Corresponding amplitude spectra. (*a*) Wavy Vortex Flow (WVF) regime. (*b*) Modulated Wavy Vortex Flow (MWVF) regime. (*c*) Chaotic Wavy Vortex Flow (CWVF) regime (*d*) Wavy Turbulent Vortex flow (WTVF) regime (*e*) Turbulent Taylor Vortex Flow (TTVF) regime. The examples here belong to the ramp-up experiment.

A comprehensive summary of the flow regimes for our experiments is shown in figure 3. The maximum Reynolds numbers achieved are $Re/Re_c = 18.58$ and 15.42 for the ramp-up and ramp-down protocols respectively. In general, it can be seen that the flow states achieved in the two protocols are not the same, implying the presence of hysteresis for the higher order transitions. We only address the key points here in the text.

For the ramp-up experiments, the first appearance of Wavy Vortex Flow is characterized by the presence of six azimuthal waves and nine vortex pairs. Even though the first non-axisymmetric mode should ideally have one azimuthal wave, and progressively rise, we do not observe it due to our finite step sizes. For example, Krueger *et al.* (1966) theoretically show for $\eta \to 1$ that the flow goes from Taylor vortex flow to Wavy vortex flow with five waves by $Re \approx 1.05Re_c$. The amplitude of these waves progressively increase with increasing Reynolds numbers (especially in the bulk), and the flow eventually appears to be in a mixed-mode state ($Re/Re_c = 2.01$). The mixed-mode state appears to be similar to the observations of Donnelly *et al.* (1980) "irregularities in the roll and wavy structure" and King & Swinney (1983) "distorted wave patterns". The mixed-mode manifests itself in the spectrum by the appearance of a peak corresponding to the azimuthal state with nine waves, which also happens to be a feature of the next flow state ($2.12 \leqslant Re/Re_c \leqslant 2.22$). At $Re/Re_c = 2.12$, a vortex pinching process is simultaneously incepted and is completed at $Re/Re_c = 2.22$. This pinching process is visible in the space-time plots as spiral defects/dislocations (not shown).

For $2.22 \leqslant Re/Re_c \leqslant 2.62$, we observe a distinct low-frequency component in the spectrum ($f/f_i < 1$), which Dutcher & Muller (2009) refer to as an "early-modulated
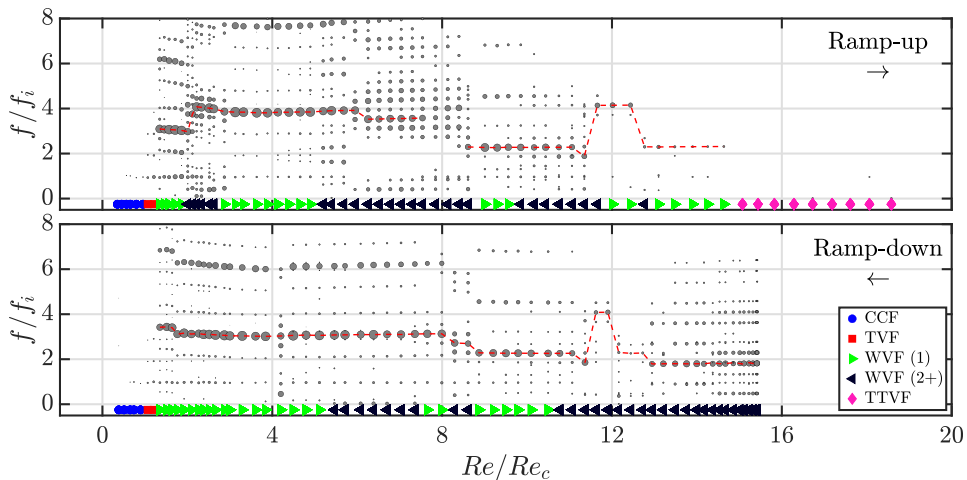
FIGURE 3. Compilation of frequency spectra for single-phase flows. The size of the markers are proportional to their amplitude in the spectrum. The coloured markers at the bottom correspond to the flow regimes shown in figure 3 of the manuscript. In the legend, WVF (1) and WVF (2+) refer to periodic (single, distinct peak in spectrum) and quasi-periodic (at least two, distinct, incommensurate peaks in spectrum) Wavy vortex flows respectively.

wavy flow" region. While they mention that such modulations were never reported for flows with a static outer cylinder, these low-frequency components appear to be very similar to "transient mode" identified by Fenstermacher *et al.* (1979). We nevertheless stick with the convention of Dutcher & Muller (2009) and classify it as a modulated wavy vortex flow (see figure 2(*b*)). The range of Reynolds numbers over which this regime is observed by us is much narrower than that of Dutcher & Muller (2009) ($1.43 \leqslant Re/Re_c \leqslant 3.56$), and we speculate that it could be attributed to the shorter aspect ratio of our system.

At $Re/Re_c = 2.87$, yet another vortex pair degenerates, and the low-frequency component disappears from the spectrum as well. The spectrum has a single, dominant frequency between $2.87 \leqslant Re/Re_c \leqslant 4.90$, and we classify it as a Wavy Vortex Flow. This second appearance of the Wavy Vortex Flow was also observed by Dutcher & Muller (2009) ($3.56 \leqslant Re/Re_c \leqslant 5.20$), and implicitly by Fenstermacher *et al.* (1979). Between $5.20 \leqslant Re/Re_c \leqslant 5.68$, a second frequency component ($f/f_i > 1$) appears, what we classify as a Modulated Wavy Vortex Flow. Dutcher & Muller (2009) too observe this regime with $f/f_i > 1$. Hereafter, the region of $5.95 \leqslant Re/Re_c \leqslant 8.61$ is characterized by the presence of a spectrum with multiple peaks and making a clear classification cannot be done until a systematic distinction between the significance of the different peaks is performed. However, we do observe that beyond $Re/Re_c = 7.85$, the flow appears to have a visible presence of small-scale structures and the flow may then be considered to be in the Chaotic Wavy Vortex Flow regime (see figure 2(*c*)).

At $Re/Re_c = 9.00$, we observe the Wavy Turbulent Vortex Flow (compared to $Re/Re_c = 7.85$ reported by Dutcher & Muller (2009)), which is characterized by the presence of a single, dominant peak in the spectrum, while the flow displays small-scale structures. The 'turbulence' is also evident in the noise floor of the amplitude spectrum (see figure 2(*d*)). Between $11.06 \leqslant Re/Re_c \leqslant 11.35$, a shift in the azimuthal state occurs via a spectral cascade . However, between $11.66 \leqslant Re/Re_c \leqslant 12.44$, a peculiar shift in the temporal frequencies is observed. The frequency peak corresponding to the Wavy Turbulent Vortex Flow disappears suddenly, and is replaced by a high frequency

component ($f/f_i > 4$). At first sight, this regime seems to qualitatively resemble the 'Fast Azimuthal Wave' (Walden & Donnelly 1979; Takeda 1999). However, a key difference is that the fast azimuthal wave appears only once the Turbulent Taylor Vortex Flow has set in, usually $Re/Re_c \geqslant 23$ (Takeda 1999). The Wavy Turbulent Vortex Flow then returns for $12.77 \leqslant Re/Re_c \leqslant 14.63$, before giving way to Turbulent Taylor Vortex Flow for $15.07 \leqslant Re/Re_c \leqslant 18.58$ with an axial wavelength of $\approx 2.78d$. Dutcher & Muller (2009) report the onset of Turbulent Taylor Vortex flow at $Re/Re_c = 15.4$. It must be noted that Dutcher & Muller (2009) also report the appearance and subsequent disappearance of second temporal frequencies beyond the wavy Turbulent vortex Flow. Such an observation is indicative of the fact that the exact nature of higher order transitions is not necessarily set in stone, and the analysis may thus be subjective.

The ramp-down experiments evidently show a different behaviour (see figure 3). One key observation is that we do not access the Turbulent Taylor Vortex Flow regime. Possible reasons for this may include: we accessed relatively lower Reynolds numbers owing to higher temperatures, and the high acceleration rate to reach the highest shear rate may delay the critical Reynolds number (see Dutcher & Muller 2009). Instead, at the highest Reynolds number of $Re/Re_c = 15.41$, we observe a Wavy state with at least two incommensurate frequencies. Since the flow also shows distinct small-scale features, we classify it as a Chaotic Wavy Vortex Flow regime. This behaviour continues for the range $15.41 \geqslant Re/Re_c \geqslant 12.94$ with the exception of $Re/Re_c = 13.21$, where the frequency of the second wave appears to be different. A vortex pair disappears at $Re/Re_c = 12.72$ and between $12.72 \geqslant Re/Re_c \geqslant 12.16$, the nature of the flow remains Chaotic Wavy, but where the frequencies involved are markedly different, with drastically reduced amplitudes in the spectrum. This then gives way to a regime ($11.90 \geqslant Re/Re_c \geqslant 11.62$) resembling the 'Fast Azimuthal Wave' ($f/f_i > 4$) that was also observed in the ramp-up experiments.

Between $11.36 \geqslant Re/Re_c \geqslant 7.99$, the flow goes from Chaotic Wavy Vortex Flow to a Modulated Wavy Vortex Flow state via a couple of transitions in the azimuthal state ($11.36 \geqslant Re/Re_c \geqslant 11.06$ and $8.87 \geqslant Re/Re_c \geqslant 7.99$). The Modulated Wavy Vortex Flow between $7.65 \geqslant Re/Re_c \geqslant 5.46$ is characterized by a very low-frequency component. Hereafter, the Wavy Vortex Flow is recovered for the region $5.11 \geqslant Re/Re_c \geqslant 1.76$, accompanied by the destruction of a vortex pair at $Re/Re_c = 4.20$. Between $1.76 \geqslant Re/Re_c \geqslant 1.64$, the Wavy Vortex Flow gains a vortex pair and is the final higher order transition.

In summary, on the basis of our ramp-up experiments, we can confidently claim that our Taylor-Couette system can reproduce flow states corresponding to higher order transitions, in agreement with those reported in literature. The results of the ramp-down experiments (in comparison to the ramp-up experiments), unsurprisingly, hint at the non-uniqueness of the flow states attained at a given Reynolds number, even from a purely topological perspective. This is unsurprising, in light of the seminal work of Coles (1965).

2. Torque data

Torque measurements provide insight into the global behaviour of the flow, since it refers to an integral quantity. For the range of Reynolds numbers considered in this study, the primary insights attainable from the torque measurements are the critical Reynolds number where the flow veers away from purely azimuthal flow. For a purely azimuthal flow, an analytical solution may be easily derived relating the skin friction coefficient
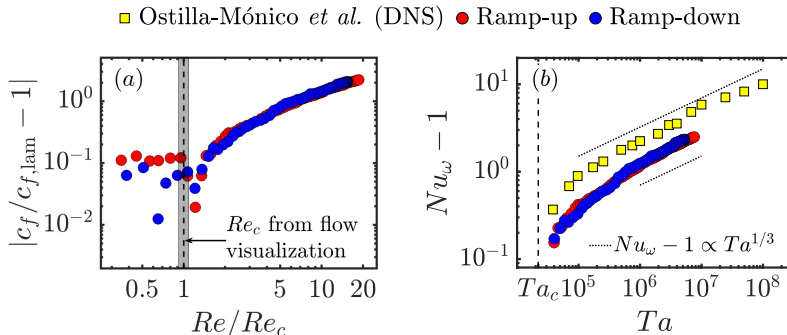
FIGURE 4. Torque measurements for both protocols are compared against numerical simulations (data from Ostilla-Mónico *et al.* 2014, figure 4(*a*), $\eta = 0.909$). (*a*) Reduced skin friction coefficient versus reduced Reynolds number. (*b*) $Nu_\omega - 1$ versus Ta.

and the Reynolds number as $c_{f,\text{lam}} = \frac{4}{\eta(1+\eta)}/Re$ (derivations available in Wendt 1933; Koeltzsch *et al.* 2003).

In figure 4(*a*), the reduced skin friction coefficient ($c_f/c_{f,\text{laminar,analytical}} - 1$) is plotted against the normalized Reynolds number. The deviation of the skin friction coefficient from its laminar value can also be used an indicator of the onset of Taylor vortices. Without any prior knowledge of the flow regime, one might over-predict Re_c by about 20%. This can be inferred by selecting the Re above which there is a monotonic rise in the reduced skin friction coefficient. Possible reasons for this over-prediction include the finite step sizes in the shear rates, as well as the measured torque values being close to the absolute resolution of the system (0.01 Nm). For this reason, the reduced skin friction coefficient does not converge to zero for $Re/Re_c < 1$ either.

To check the fidelity of the torque measurements for higher Reynolds numbers, we compare our results against those obtained in the direct numerical simulations of Ostilla-Mónico *et al.* (2014), albeit with $\eta = 0.909, \Gamma = 2\pi$. A clear difference is visible in the comparison of $Nu_\omega - 1$ versus Ta, in terms of the absolute values, but the profile shapes appear to be very similar. The differences in the absolute values may be attributed to differing boundary conditions (the numerical simulations do not simulate end plates), as well as the difference in axial wavelengths of the Taylor rolls. For the numerical work, it has been shown that up to 20% variation in Nu_ω can be observed by changing the axial wavelength of the Taylor vortices, especially at low Ta (Ostilla *et al.* 2013, their section 3.4). Moreover, for $Re > 400$, the global scaling behaviour of $G \propto Re^{1.47}$ (alternatively, $G \propto Re^{1.49}$) was seen for the ramp-up (ramp-down) experiments. The scaling exponents are in close agreement with the exponent of 1.5 available in the empirical correlations of Wendt (1933). The value of 1.5 is attributed to the dominance of boundary layer and hairpin contributions (Eckhardt *et al.* 2007). In summary, our results suggest that our torque measurements are reliable for commenting on global scaling behaviours.

REFERENCES

ALIDAI, A., GREIDANUS, A. J., DELFOS, R. & WESTERWEEL, J. 2016 Turbulent Spot in Linearly Stable Taylor Couette Flow. *Flow, Turbulence and Combustion* **96** (3), 609–619.

COLE, J. A. 1976 Taylor-vortex instability and annulus-length effects. *Journal of Fluid Mechanics* **75** (1), 1–15.

COLES, D. 1965 Transition in circular Couette flow. *Journal of Fluid Mechanics* **21** (3), 385–425.

CZARNY, O. & LUEPTOW, R. M. 2007 Time scales for transition in Taylor–Couette flow. *Physics of Fluids* **19** (5), 054103.

DI PRIMA, R. C. & SWINNEY, H. L. 1981 Instabilities and transition in flow between concentric rotating cylinders. In *Hydrodynamic instabilities and the transition to turbulence*, pp. 139–180. Springer.

DONNELLY, R. J., PARK, K., SHAW, R. & WALDEN, R. W. 1980 Early nonperiodic transitions in Couette flow. *Physical Review Letters* **44** (15), 987.

DUTCHER, C. S. & MULLER, S. J. 2009 Spatio-temporal mode dynamics and higher order transitions in high aspect ratio Newtonian Taylor–Couette flows. *Journal of Fluid Mechanics* **641**, 85–113.

ECKHARDT, B., GROSSMANN, S. & LOHSE, D. 2007 Torque scaling in turbulent Taylor–Couette flow between independently rotating cylinders. *Journal of Fluid Mechanics* **581**, 221–250.

ESSER, A. & GROSSMANN, S. 1996 Analytic expression for Taylor–Couette stability boundary. *Physics of Fluids* **8** (7), 1814–1819.

FENSTERMACHER, P. R., SWINNEY, H. L. & GOLLUB, J. P. 1979 Dynamical instabilities and the transition to chaotic Taylor vortex flow. *Journal of Fluid Mechanics* **94** (1), 103–128.

GORMAN, M., REITH, L. A. & SWINNEY, H. L. 1980 Modulation patterns, multiple frequencies, and other phenomena in circular Couette flow. *Annals of the New York Academy of Sciences* **357** (1), 10–21.

JONES, C. A. 1985 The transition to wavy Taylor vortices. *Journal of Fluid Mechanics* **157**, 135–162.

KING, G. P., LI, Y., LEE, W., SWINNEY, H. L. & MARCUS, P. S. 1984 Wave speeds in wavy Taylor-vortex flow. *Journal of Fluid Mechanics* **141**, 365–390.

KING, G. P. & SWINNEY, H. L. 1983 Limits of stability and irregular flow patterns in wavy vortex flow. *Physical Review A* **27** (2), 1240.

KOELTZSCH, K., QI, Y., BRODKEY, R. S. & ZAKIN, J. L. 2003 Drag reduction using surfactants in a rotating cylinder geometry. *Experiments in Fluids* **34** (4), 515–530.

KRUEGER, E. R., GROSS, A. & DI PRIMA, R. C. 1966 On the relative importance of Taylor-vortex and non-axisymmetric modes in flow between rotating cylinders. *Journal of Fluid Mechanics* **24** (3), 521–538.

LUEPTOW, R. M., DOCTER, A. & MIN, K. 1992 Stability of axial flow in an annulus with a rotating inner cylinder. *Physics of Fluids A: Fluid Dynamics* **4** (11), 2446–2455.

OSTILLA, R., STEVENS, R. J. A. M., GROSSMANN, S., VERZICCO, R. & LOHSE, D. 2013 Optimal Taylor–Couette flow: direct numerical simulations. *Journal of Fluid Mechanics* **719**, 14–46.

OSTILLA-MÓNICO, R., HUISMAN, S. G., JANNINK, T. J. G., VAN GILS, D. P. M., VERZICCO, R., GROSSMANN, S., SUN, C. & LOHSE, D. 2014 Optimal Taylor–Couette flow: radius ratio dependence. *Journal of Fluid Mechanics* **747**, 1–29.

RAVELET, F., DELFOS, R. & WESTERWEEL, J. 2010 Influence of global rotation and Reynolds number on the large-scale features of a turbulent Taylor–Couette flow. *Physics of Fluids* **22** (5), 055103.

TAKEDA, Y. 1999 Quasi-periodic state and transition to turbulence in a rotating Couette system. *Journal of Fluid Mechanics* **389**, 81–99.

TAKEDA, Y., FISCHER, W. E., SAKAKIBARA, J. & OHMURA, K. 1993 Experimental observation of the quasiperiodic modes in a rotating Couette system. *Physical Review E* **47** (6), 4130.

WALDEN, R. W. & DONNELLY, R. J. 1979 Reemergent order of chaotic circular Couette flow. *Physical Review Letters* **42** (5), 301.

WENDT, F. 1933 Turbulente Strömungen zwischen zwei rotierenden konaxialen Zylindern. *Archive of Applied Mechanics* **4** (6), 577–595.